Materials Science & Engineering C 117 (2020) 111279

Contents lists available at ScienceDirect

Materials Science & Engineering C

journal homepage: www.elsevier.com/locate/msec

Formulation, characterization and *in vitro* anti-leishmanial evaluation of amphotericin B loaded solid lipid nanoparticles coated with vitamin B_{12}-stearic acid conjugate

Aakriti Singh[a,1], Ganesh Yadagiri[a,1], Shabi Parvez[a], Om Prakash Singh[b], Anurag Verma[d], Shyam Sundar[c], Shyam Lal Mudavath[a,*]

[a] Infectious Disease Biology Laboratory, Chemical Biology Unit, Institute of Nano Science & Technology, Habitat Centre, Phase 10, Sector 64, Mohali, Punjab 160062, India
[b] Department of Biochemistry, Institute of Science, Banaras Hindu University, Varanasi, Uttar Pradesh 221005, India
[c] Infectious Disease Research Laboratory, Department of Medicine, Institute of Medical Sciences, Banaras Hindu University, Varanasi, Uttar Pradesh 221005, India
[d] School of Pharmaceutical Sciences, IFTM University, Moradabad, Uttar Pradesh 244001, India

ARTICLE INFO

Keywords:
Vitamin B_{12}-stearic acid conjugate
Solid lipid nanoparticles
Amphotericin B
Visceral leishmaniasis

ABSTRACT

Despite the advancement of new anti-leishmanials, amphotericin B (AmB) prevails as one of the most potent agent in the treatment of visceral leishmaniasis (VL), a neglected tropical disease affecting mostly poverty ridden and underdeveloped regions of the globe. Nonetheless, many patients display intolerance to parenteral AmB, notably at higher dosages. Also, conventional AmB presents an apparently poor absorption. Therefore, to improve AmB bioavailability and overcome multiple barriers for oral delivery of AmB, we fabricated a promising vitamin B_{12}-stearic acid (VBS) conjugate coated solid lipid nanoparticles (SLNs) encapsulated with AmB (VBS-AmB-SLNs) by a combination of double emulsion solvent evaporation and thermal sensitive hydrogel techniques. VBS-AmB-SLNs showed a particle size of 306.66 ± 3.35 nm with polydispersity index of 0.335 ± 0.08 while the encapsulation efficiency and drug loading was observed to be 97.99 ± 1.6% and 38.5 ± 5.6% respectively. *In vitro* drug release showed a biphasic release pattern and chemical stability of AmB was ensured against simulated gastrointestinal fluids. Cellular uptake studies confirmed complete internalization of the formulation. Anti-leishmanial evaluation against intramacrophage amastigotes showed an enhanced efficacy of 94% which was significantly ($P < 0.01$) higher than conventional AmB without showing any toxic effects on J774A.1 cells. VBS-AmB-SLNs could serve as a potential therapeutic strategy against VL.

1. Introduction

Visceral leishmaniasis (VL) is one of the most neglected tropical disease caused by protozoan parasite *Leishmania donovani*, an insidious parasite that is transmitted by the bite of an infected sand fly [1]. VL affects mainly poor and malnourished people in under developed countries of Brazil, East Africa and South-East Asia. According to World Health Organisation (WHO), 50,000–90,000 new VL cases were reported globally and more than 95% of new VL cases were reported in 10 countries: Bangladesh, Brazil, China, Ethiopia, India, Kenya, Nepal, Somalia, South Sudan and Sudan. Clinical manifestations of VL include hepato-splenomegaly, irregular bouts of fever, weight loss, anaemia and even causes death if left untreated [2]. Current anti-leishmanial drug therapies lead to severe toxic side effects and non-availability of proper vector control measures and effective vaccine(s) against VL along with development of drug resistant parasites creates a big hurdle to VL treatment and control [3]. Emergence of drug resistant parasites and HIV-VL co-infections are vital factors behind VL treatment failure. Soon after discovery of *Leishmania* parasite as a causative agent for VL, pentavalent antimonials (sodium stibogluconate and meglumine antimonite) were the mainstay of therapy for VL, however in Indian subcontinent, sodium stibogluconate was no longer recommended for clinical use because of its drug resistance. In early 1980s, VL patients showed resistance even to very small doses and shorter duration of treatment with pentavalent antimonials (10 mg/kg for 6–10 days) and in later years, it showed treatment failure even at higher doses (20 mg/kg) for longer duration [4,5]. Emergence of drug resistance to sodium stibogluconate in Indian subcontinent resulted in the recommendation

* Corresponding author.
E-mail addresses: shyamlal@inst.ac.in, shavs0502@gmail.com (S.L. Mudavath).
[1] Authors contributed equally.

https://doi.org/10.1016/j.msec.2020.111279
Received 16 January 2020; Received in revised form 7 June 2020; Accepted 6 July 2020
Available online 09 July 2020

of amphotericin B (AmB) as a first-line treatment option in kala-azar infected patients. However, infusion-related fever, chills and rigour are some of the common side effects with parenteral administration of AmB, and lethal adverse effects include hypokalaemia, nephrotoxicity and myocarditis, which requires continuous monitoring and prolonged hospitalisation of patient and increases the cost of therapy [6–8].

The prime reason of compelling intravenous administration is the low fraction of AmB that is orally absorbed (0.2–0.9%) due to the precipitation of crystalline drug in aqueous media. The zwitter ionic and amphiphilic character of AmB with an asymmetrical distribution of ionisable carboxyl, primary amine groups, hydrophobic and hydrophilic groups respectively corresponds to poor aqueous solubility (< 1 mgL^{-1} at physiological pH) [9–11]. Thus, to achieve clinically effective AmB concentrations in targeted organs after oral administration, chemical modification of the drug or reformulation using appropriate excipients is required.

Oral drug delivery is the most desirable delivery route being non-invasive, convenient and cost effective. Solubility is a principal aspect culpable for the low bioavailability of drugs administered orally; encapsulation in a drug delivery system that has the competence to armor a molecule's hostile physicochemical characteristics and can contribute to become a viable solution. Stability in acidic gastric environment and protection from enzyme degradation are also key requirements. The advancement of a conducive oral formulation of drugs must balance the need to boost absorption and safeguard the acid-labile molecule from degradation in the gastric environment with the requisite release of the drug at target site in a monomeric form [12].

Consequently, innovations in the field of nanotechnology have overcome certain limitations along with attaining an increased efficacy. Therefore, to significantly reduce the incidence of the disease there is an immediate requirement for a modified drug delivery system which encapsulate drugs, while minimizing toxic effects to normal cells [12–14]. Among several carrier systems developed, solid lipid nanoparticles (SLNs) provide unique potential in drug delivery applications with enhanced properties like higher stability and high drug loading. They are considered to be the most effective biodegradable lipid based colloidal carriers, which incorporate and hence provide an improved bioavailability and extended residence time of poorly water soluble drugs [15].

Stearic acid, a saturated fatty acid is generally regarded as safe (GRAS) lipid and has been extensively used in drugs, food, and cosmetics. Stearic acid used in the preparation of SLNs enhanced oral bioavailability and safety [16]. Stearic acid–octaarginine modified SLNs were effectively used for the oral administration of insulin [17]. Therefore, stearic acid was conjugated with vitamin B_{12} to achieve an augmented absorption of SLNs [18]. Vitamin B_{12} (VB_{12}) is a natural molecule which has been used to improve the absorption of biomolecules and avert the exploitation of absorption enhancers and accomplish definite absorption of macromolecules. Further, surface modification with VB_{12}-stearic acid conjugate improves absorption in small intestine by an intricate receptor mediated uptake pathway present in our body. Endocytosis of conjugated form of VB_{12} enhances the membrane transport efficiency to the target cell thereby indirectly achieving enhanced targetability and bioavailability of drugs [19–24].

Herein, we have formulated a novel nanoparticulate system of VB_{12}-stearic acid conjugate coated SLNs encapsulated with AmB (VBS-AmB-SLNs) to improve AmB oral absorption and enhance the anti-leishmanial efficacy and safety. To the best of our knowledge, there is no study reported by using VB_{12}-stearic acid conjugate coated SLNs as a carrier for AmB as a potential therapeutic strategy against VL.

2. Materials and methods

2.1. Chemicals

Pluronic F127, VB_{12}, AmB, 4′, 6-diamidino-2-phenylindole (DAPI), fluorescein isothiocyanate isomer I (FITC) were procured from Sigma Aldrich, U.S.A. Stearic acid, 1-ethyl-3-(3-dimethylaminopropyl) carbodiimide (EDC), oxyma, sodium bicarbonate, potassium bromide, phosphotungstic acid (PTA), solutol HS 15 and cellulose dialysis tube were obtained from HiMedia Laboratories, Mumbai, India. Glass bottom dishes were obtained from Thermo-scientific USA. Glyceryl palmitostearate (Precirol® ATO 5) was kindly provided by Gattefossét Company (Germany). Carbon-coated TEM grids were procured from Beta Tech Equipment Pvt. Ltd., India.

2.2. Synthesis of vitamin B_{12} stearate

VB_{12} was esterified to stearic acid in water containing solvent system according to slight modifications to a previously reported oxyma method [25]. Briefly, 1 mM of stearic acid was dissolved in 5% water-acetonitrile solvent system followed by the addition of 1 mM of VB_{12}. Then, 1.5 mM EDC hydrochloride, 1.5 mM oxyma and 6 mM sodium bicarbonate were added. The mixture was continuously agitated for 12 h at room temperature. After agitation, vitamin B_{12} stearate (VBS) was separated from the mixture by silica gel column chromatography (methanol:acetic ether; 60:40). The solvents were evaporated by rota evaporator and dried for 72 h in vacuum oven. The dried VBS was used in further studies.

2.3. Preparation of drug encapsulated vitamin B_{12} stearate modified solid lipid nanoparticles

Vitamin B_{12} stearate modified solid lipid nanoparticles encapsulated with AmB (VBS-AmB-SLNs) were prepared by slight modifications of a previously reported method [26]. AmB (50 mg) was dissolved in 40% pluronic F127 HCl solution. Simultaneously, VBS (24 mg), glycerol monostearate (30 mg) and Precirol® ATO 5 (60 mg) were dissolved in dichloromethane firstly by stirring for 30 min and then *via* sonication for 5 min at room temperature. The dispersion was then transferred to 300 mg of mixture containing AmB in pluronic F127 solution. This system was sonicated for 10 min to form primary gel in oil emulsion which was further transferred to 2% solutol solution preheated to 37 °C and stirred for 30 min followed by sonication for 10 min at 4 °C to form gel in oil in water emulsion. Finally, after dilution with 0.2% solutol the solution was stirred overnight at room temperature, allowing the formation of SLNs. The dispersion was centrifuged at 10,000 rpm for 30 min and the pellet obtained was washed three times with milli-Q water to remove any unbound drug molecules. The freshly synthesized VBS-AmB-SLNs were freeze dried (FDUT-12003, Republic of Korea) and used for further studies. Plain VBS coated solid lipid nanoparticles (VBS-PSLNs) were also prepared using the same method as mentioned above without adding AmB. Here, VBS (8 mg), glycerol monostearate (10 mg) and Precirol® ATO 5 (20 mg) were dissolved in dichloromethane firstly by stirring for 30 min and then *via* sonication for 5 min at room temperature. The dispersion was then transferred to 100 mg of 40% pluronic F127 solution and the above mentioned procedure was repeated to obtain freeze dried VBS-PSLNs.

2.4. Entrapment efficiency and drug loading

The AmB content was determined by using an indirect method with slight modifications [27]. Briefly, the dispersion of VBS-AmB-SLNs was centrifuged at 10,000 rpm for 30 min and the supernatant obtained was analyzed using UV–visible spectrophotometer (Shimadzu, UV-2600) at 405 nm. The encapsulation efficiency and drug loading were determined by using the following formulae.

$$(\%EE) = \frac{\text{total amount of drug} - \text{amount of free drug in supernatant}}{\text{total amount of drug}} \times 100$$

$$(\%DL) = \frac{\text{total amount of drug} - \text{amount of free drug}}{\text{total amount of formulation components}} \times 100$$

2.5. Characterization

2.5.1. Fourier-transform infrared spectroscopy (FTIR)

The formation of synthesized derivative VBS was confirmed by FTIR spectroscopy (Agilent Cary 620 FTIR spectroscopy). The samples were prepared in potassium bromide (KBr) pellets and individual spectrum was obtained in the region between 4000 and 500 cm^{-1}.

2.5.2. X-ray diffraction (XRD)

X-ray diffractogram of AmB, VB_{12} and VBS-AmB-SLNs was obtained using X-ray diffractometer (Bruker, D8 Advance X-ray Diffractometer) equipped with Cu-Kα radiation source (λ = 1.541 Å). The instrument was fixed at 40 kV, 25 mA and the diffraction angle (2θ) was measured from 5° to 50°.

2.5.3. Particle size and zeta potential

Particle size and zeta potential was assessed by dynamic light scattering using Zetasizer (Malvern, Nano ZS90, UK) at 25 °C and all the experiments were done in triplicate. Briefly, the samples were diluted (1:10) with milli-Q water and placed in polystyrene disposable cuvettes (Model-DTS0012; Malvern) for the measurement of particle size and in disposable folded capillary cells (Model-DTS1070; Malvern) for measurement of zeta potential.

2.5.4. Electron microscopy

The morphology of VBS-PSLNs and VBS-AmB-SLNs were analyzed by scanning electron microscopy (SEM; IT300, JEOL 6400, JEOL USA, Peabody, MA.) and transmission electron microscopy (TEM; JEOL 2100, Country). For SEM, freeze dried samples were diluted (1:10), drop casted on a cover slip and air dried followed by sputter coating with colloidal gold under vacuum using JEC-300FC. TEM images were obtained at an accelerating voltage of 200 kV having lanthanum hexaboride (LaB6) filament. TEM micrographs were captured using Gatan camera software. For TEM, freeze dried samples were diluted (1:10), drop casted on to copper grid and allowed to air dry at room temperature. The samples were negatively stained with 2% w/v PTA and washed thrice with milli-Q water followed by overnight vacuum drying.

2.6. In vitro release study

The release of AmB from VBS-AmB-SLNs was analyzed using dialysis method. VBS-AmB-SLNs were introduced into pre-soaked cellulose dialysis membrane (12 kDa) and dialyzed against 30 ml of phosphate buffer solution (PBS; pH 7.4) containing 1% tween® 80 maintained at 37 ± 2 °C with continuous stirring at 100 rpm for 48 h. Aliquots were withdrawn at pre-determined time intervals, replaced with fresh buffer to maintain sink condition and analyzed using UV–visible spectroscopy (Shimadzu UV-2600) at 405 nm.

2.7. Stability study: in-vitro release in simulated gastro-intestinal fluid

In vitro simulated gastric fluid (SGF) and simulated intestinal fluid (SIF) medium with enzymes were prepared and release experiments were performed. VBS-AmB-SLNs were placed in hydroxypropyl methylcellulose (HPMC) capsule and placed in separate dissolution baskets containing 500 ml of simulated gastric fluid (pH 1.6) and 500 ml of simulated intestinal fluid (pH 6.8) at 37 ± 0.5 °C with continuous stirring at 50 rpm. The SGF was prepared by adding lecithin (20 μM), pepsin (0.1 mg/ml), sodium chloride (34.2 mM), sodium taurocholate (80 μM) and HCl conc. (*q.s.* pH 1.2) in 500 ml deionised water while SIF was prepared by adding sodium taurocholate (3 mM), lecithin (0.75 mM), sodium di-hydrogen phosphate (3.43 g), sodium chloride (6.18 g) and sodium hydroxide (*q.s.* pH 6.5) in 500 ml deionised water [28]. Samples were withdrawn at regular time intervals, and amount of drug in the supernatant was analyzed by using a UV–visible spectrophotometer (Shimadzu, UV-2600) at 405 nm.

2.8. Mucoadhesive capacity

A turbidimetric analysis was performed in order to indirectly determine the interaction between mucin and VBS-AmB-SLNs according to slight modifications of a previously reported method [27]. Briefly, a fresh solution of mucin (0.1%, w/v) isolated from porcine stomach (type II) was placed in an incubation chamber where 80–90% relative humidity and 37 ± 2 °C was maintained with continuous shaking. 10 mg of VBS-AmB-SLNs was added into 10 ml of aqueous mucin dispersion and stirred at 200 rpm for 4 h to ensure that the SLNs were able to form bioadhesion with mucin. The turbidity of dispersion was measured at regular time intervals and compared with the turbidity of the native mucin dispersion which served as control using a UV–visible spectrophotometer (Shimadzu, UV-2600) at 650 nm. All experiments were performed in triplicate.

2.9. Cell line and parasite

The J774A.1 macrophage cell line was obtained from the National Centre for Cell Science, Pune, India. The J774A.1 cells were cultured in Roswell Park Memorial Institute 1640 media (RPMI 1640; Gibco, ThermoFisher Scientific) supplemented with 10% heat inactivated fetal bovine serum (HIFBS; Gibco, ThermoFisher Scientific), 1% Penicillin/Streptomycin (Pen/Strep, 10,000 IU/ml; Gibco, ThermoFisher Scientific), sodium bicarbonate (Sodium Bicarbonate Solution, Gibco, ThermoFisher Scientific) and HEPES (Gibco HEPES, ThermoFisher Scientific). The cells were maintained in a humidified incubator at 37 °C with 5% CO_2 environment. For, *in vitro* anti-leishmanial activity, *Leishmania donovani* (LEM 138) parasites were cultured in M199 medium supplemented with 10% heat-inactivated foetal bovine serum (HIFBS), gentamycin (50 μg/ml) and penicillin streptomycin (100 μg/ml) and maintained at 26 °C in a BOD incubator.

2.10. In vitro cytotoxicity assay

The cytotoxicity of VBS-AmB-SLNs was assessed by using 3-(4,5-dimethylthiazol-2-yl)-2,5-diphenyltetrazolium bromide (MTT) assay on J774A.1 macrophage cell line. Briefly, J774A.1 cells were seeded in 96 well plates at an initial cell density of 5×10^4 cells/well and incubated for 24 h at 37 °C and 5% CO_2 environment allowing the cells to adhere. The cells were treated in triplicate with varying concentrations of VBS-AmB-SLNs (500 μg/ml–0.5 μg/ml) for 24 h at 37 °C, 5% CO_2; untreated cells served as a control. After treatment, a volume of 20 μl MTT reagent (5 mg/ml) was added to each well and incubated for 4 h to form reduced MTT formazan crystals. The precipitated crystals were dissolved in 100 μl of dimethyl sulfoxide (DMSO). Finally, the reduced MTT was spectrophotometrically analyzed at 570 nm, using a microplate reader (Infinite 200 PRO microplate plate reader). The percentage viability was expressed as percentage of $[1 - (OD_{control} - OD_{SLNs}) / (OD_{control} - OD_{blank})] \times 100$.

2.11. Cellular uptake study

FITC labeled VBS-AmB-SLNs were prepared by slight modifications of a previously reported method [29]. Briefly, 5×10^4 J774A.1 cells were seeded onto glass bottom dishes (Nunc, Thermo scientific, USA) and allowed to adhere for 24 h at 37 °C with 5% CO_2 environment. The cells were washed with incomplete RPMI-1640 media and treated with 50 μM FITC labeled VBS-SLNs for 24, 48 and 72 h. After treatment, cells were fixed with 4% paraformaldehyde for 20 min followed by washing three times with 1× PBS. The cells were then stained with DAPI for

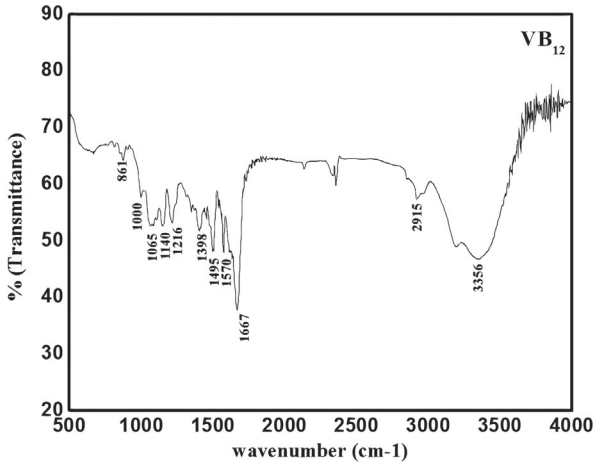

(a): FTIR spectrum of VB_{12}.

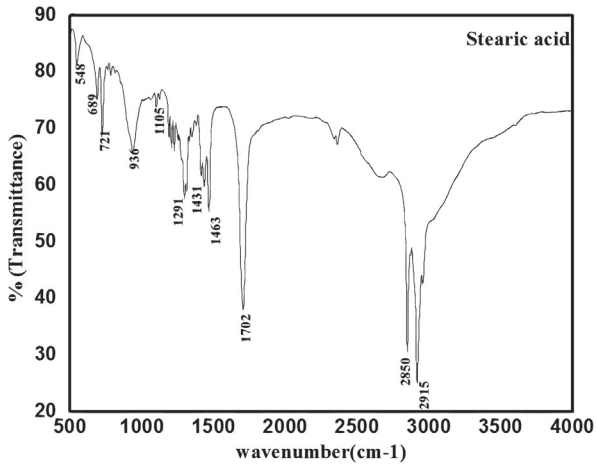

(b): FTIR spectrum of stearic acid.

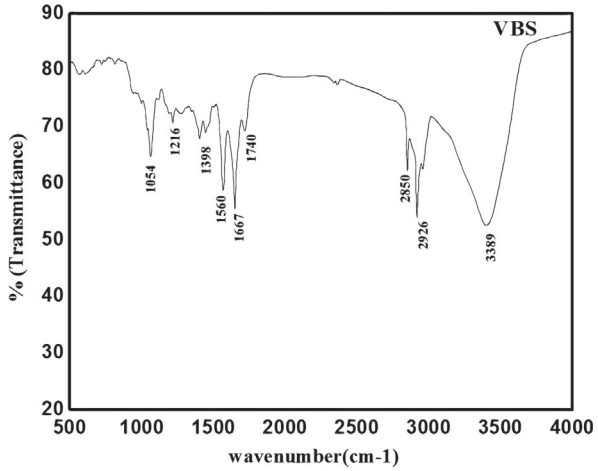

(c): FTIR spectrum of VBS.

Fig. 1. (a): FTIR spectrum of VB_{12}.
(b): FTIR spectrum of stearic acid.
(c): FTIR spectrum of VBS.

5 min followed by washing three times with 1× PBS. The images were acquired at 63× using confocal laser scanning microscope (CLSM, LSM 880 NLO, Carl Zeiss, Germany).

2.12. In vitro anti-leishmanial activity of VBS-AmB-SLNs against intracellular amastigotes of L. donovani

In vitro anti-leishmanial activity of VBS-AmB-SLNs was performed against intracellular amastigotes of *L. donovani*. Briefly, J774A.1 macrophage (2.5×10^4 cells/ml) were cultured in complete RPMI-1640 and seeded (200 µl/well) in eight chamber Lab Teck tissue culture slides (Nunc, USA) followed by incubation at 37 °C and 5% CO_2 environment for 2 h, allowing the cells to adhere. The adherent macrophages were washed three times with pre-warmed incomplete RPMI-1640 and infected with metacyclic promastigotes in 1:10 ratio, followed by incubation at 37 °C and 5% CO_2 environment for 12 h. Non-phagocytosed promastigotes were removed by washing three times with warm incomplete RPMI-1640 and the infected macrophages were incubated in the presence and absence of test and reference drugs (VBS-AmB-SLNs, VBS-PSLNs, and AmB) in different concentrations (0.1–1 µg/ml) in complete RPMI-1640 at 37 °C and 5% CO_2 atmosphere for 72 h. The infected macrophages were washed with PBS and stained with wright's stain to assess the intra-cellular amastigote growth. The intra-cellular amastigotes were monitored by counting at least 100 cells per slide under oil immersion lens microscope (100×) [1,30]. Percentage inhibition of amastigote multiplication was calculated by following formula:

$$PI = 100 - (AT/AC) \times 100$$

where PI is percentage inhibition of amastigote multiplication,
AT is actual number of amastigotes in treated samples/100 macrophages;
AC is actual number of amastigotes in control samples/100 macrophages.

3. Results and discussion

3.1. Synthesis and characterization of VBS

VB_{12} is a hydrophilic molecule and to adhere it onto the surface of SLNs, it was esterified with stearic acid, a long chain saturated fatty

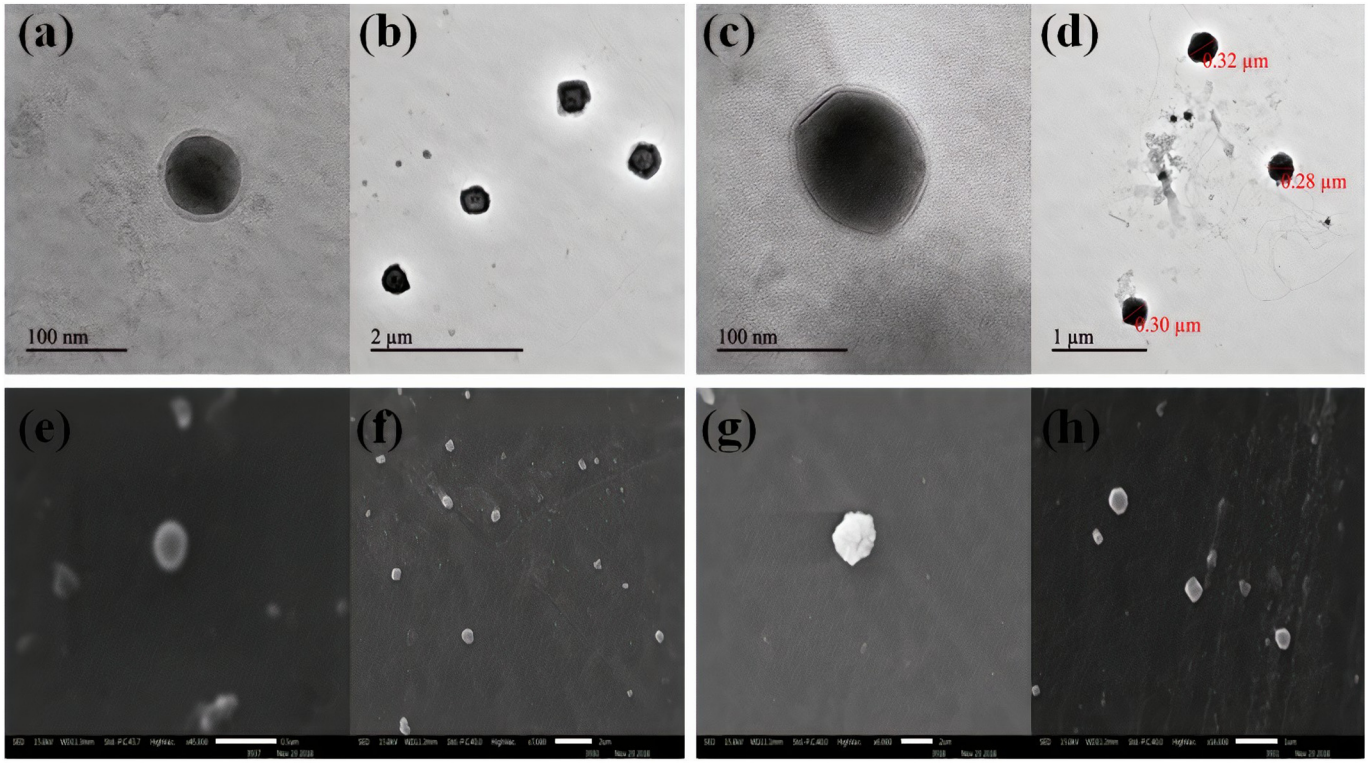

Fig. 2. TEM images of (a, b) VBS-PSLNs and (c, d) VBS-AmB-SLNs.
SEM images of (e, f) VBS-PSLNs and (g, h) VBS-AmB-SLNs.

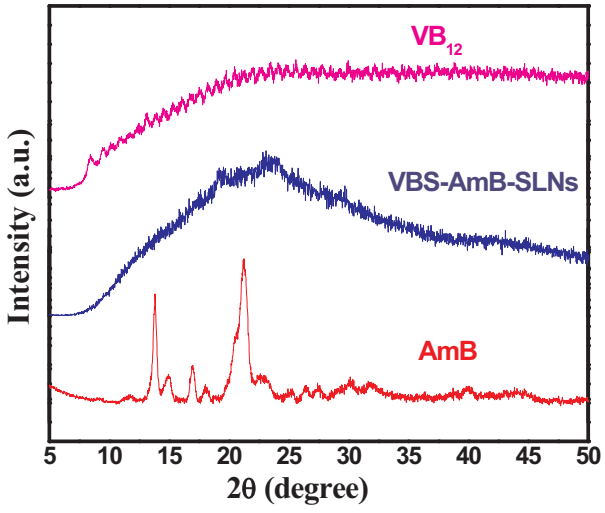

Fig. 3. X-ray diffraction (XRD) spectrum of $VB_{12,}$ VBS-AmB-SLNs and AmB.

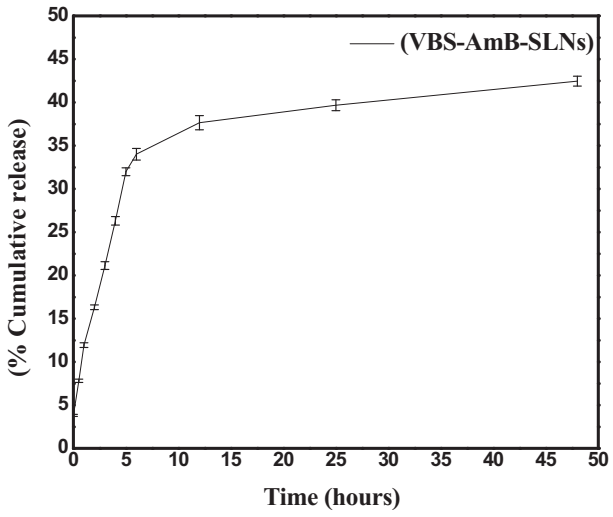

Fig. 4. *In-vitro* release profile of VBS-AmB-SLNs in PBS (pH 7.4). Results are presented as mean ± standard deviation.

acid. VBS was synthesized *via* oxyma method and characterized using Fourier-transform infrared spectroscopy. The FTIR spectra of VB_{12}, Fig. 1(a) shows a broad peak at about 3400cm^{-1} (3356 cm^{-1}) which is assigned to O–H stretching of the hydroxyl groups attached to the surface and the intense peak at around of 1667 cm^{-1} is attributed to C=O stretching vibration of propionamide side chain of VB_{12}. A medium FTIR peak at around 1570 cm^{-1} could be attributed to δ(C=C). The band at 1495 cm^{-1} could be assigned to the in-phase-stretching mode of the C=C bonds of the corrin ring [58–60]. The FTIR spectra of stearic acid Fig. 1(b) shows a carbonyl peak at 1702 cm^{-1}. The peaks at 2850 cm^{-1} and 2915 cm^{-1}are attributed to CH_2 symmetric stretch and CH_2 anti-symmetric stretch. The peaks at 940 cm^{-1}, 1105 cm^{-1}, 1291 cm^{-1} and 1463 cm^{-1} are attributed to C–OH out of plane deformation, symmetric CH_2 rock with CH_3 sided chain, C–OH stretch and CH_2 scissor vibrations respectively. In the spectrum of VBS Fig. 1(c), peaks appearing at 3389 cm^{-1}, 2850 cm^{-1}, 2926 cm^{-1}, and 1667 cm^{-1} are due to the stretching of the hydroxyl group (–OH), CH_2 symmetric stretch and CH_2 antisymmetric stretch, and C=O group in VBS. By comparing the three spectra, the formation of a new band at 1740 cm^{-1} is evident. A new event is detected after the vitamin B_{12} loading process, whereas no such peak is observed in the vitamin B_{12} and stearic acid spectra. This phenomenon can be an evidence for the conjugation of vitamin B_{12} molecules to stearic acid. This band (1740 cm^{-1}) could be attributed to the esterification of carbonyl carbon of stearic acid with primary alcohol (ribose R5' in vitamin B_{12}). The

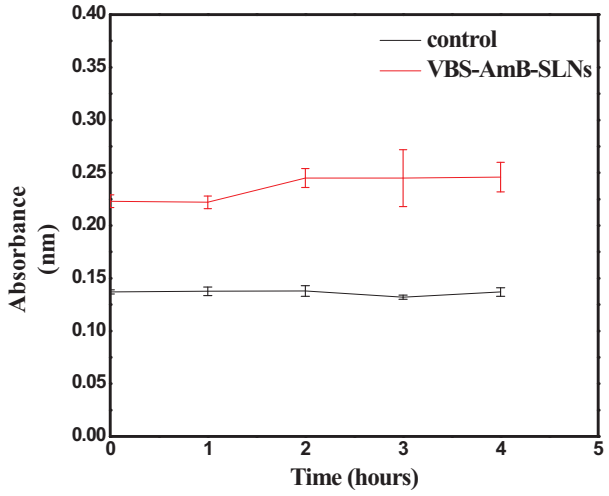

Fig. 5. Mucoadhesive measurements of VBS-AmB-SLNs using turbidimetric assay.

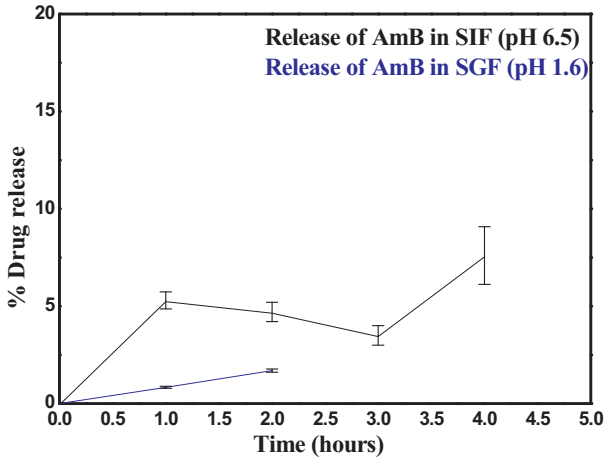

Fig. 6. *In-vitro* release profile of VBS-AmB-SLNs in SGF for 2 h and SIF for 4 h.

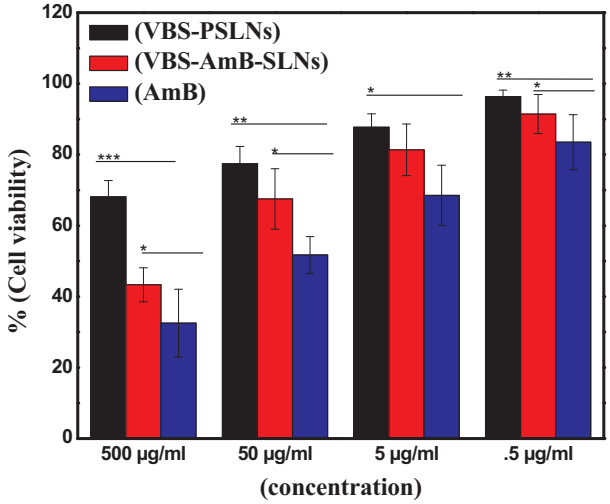

Fig. 7. Cell viability of J774A.1 cells after 24 h of incubation with VBS-AmB-SLNs at different concentration.

formation of VBS using EDC/DMAP method where similar disappearance of carboxyl vibration peak of stearic acid present at 1704 cm^{-1} was previously reported [31]. Coupled with NMR data (Supplementary information Fig. S1), we were able to confirm the formation of VBS.

3.2. Particle size and zeta potential

VBS-AmB-SLNs and VBS-PSLNs were successfully formulated by double emulsion solvent evaporation method [26]. The hydrodynamic size of VBS-PSLNs and VBS-AmB-SLNs were 101.66 ± 4.28 nm and 306.66 ± 3.35 nm with PDI values of 0.264 ± 0.02 and 0.335 ± 0.08 respectively. The particle size of VBS-AmB-SLNs was greater than VBS-PSLNs, due to encapsulation of higher amount AmB as well as simultaneous increments in quantity of surfactant providing stability and preventing agglomeration [61]. The overall particle size distribution (PDI) was less than 0.3, indicating homogeneity of synthesized SLNs. However, the zeta potential of VBS-PSLNs and VBS-AmB-SLNs was 0.152 ± 2.3 mV and 0.206 ± 2.29 mV respectively. The net neutral SLNs possess higher mucus permeating ability, which can enhance the oral bioavailability of encapsulated drugs [32].

3.3. Electron microscopy

The results of TEM and SEM imaging of VBS-PSLNs and VBS-AmB-SLNs, which are shown in Fig. 2, illustrate the fabrication of SLNs of nanometre-size spherical range and uniform size distribution. The particle size from electron microscopy accords with particle size measured by dynamic light scattering. No indication of aggregation was observed among SLNs, possibly due to steric hindrance of VB_{12} [33].

3.4. X-ray diffraction (XRD)

XRD diffraction pattern of AmB is shown in Fig. 3, exhibited sharp characteristics peaks at 2θ scattering angle of 14.1° and 21.3° which indicates its crystalline nature [34], while there was no sharp peak in VB_{12} spectra, suggesting its amorphous nature. After formulation development the characteristics peaks of AmB were either broadened and shortened suggesting the formulation turns towards amorphous form which indirectly favours the bioavailability aspect. The finding regarding the conversion of crystalline drug to amorphous state suggest appropriate drug incorporation into SLNs due to uniform distribution of AmB in the lipid matrix. Amorphous nanoparticles, serve as a source of rapidly dissolving active pharmaceutical ingredient during the absorption process when compared to its crystalline counterparts due to higher enthalpy, entropy and free energy, which could favor the bioavailability aspect [35,36].

3.5. Entrapment efficiency and drug loading

Entrapment efficiency and drug loading of an amphiphilic drug in SLNs prepared by double emulsion method was assessed by UV–Vis spectroscopy. The entrapment efficiency and drug loading of VBS-AmB-SLNs was 97.99 ± 1.6% and 38.5 ± 5.6% respectively. Due to the unique composition of SLNs matrix, it was able to form hydrophobic as well as hydrophilic interactions with AmB leading to increased lipophilicity which attributes to its high encapsulation and loading capacity [37]. It has been previously reported that the formation of ion-pairs with doxorubicin and monoalkyl phosphate esters resulted in higher incorporation of drug due to an increase in lipophilicity [38].

3.6. In-vitro release study

In vitro release of AmB from VBS-AmB-SLNs was performed using dialysis bag diffusion method in release media of pH 7.4 respectively maintained at 37 °C under continuous shaking. Drug release kinetics is a key parameter used to assess product safety and efficacy. The release profile as shown in Fig. 4, exhibits a biphasic release pattern *i.e.* an initial burst release followed by a sustained release. The initial burst

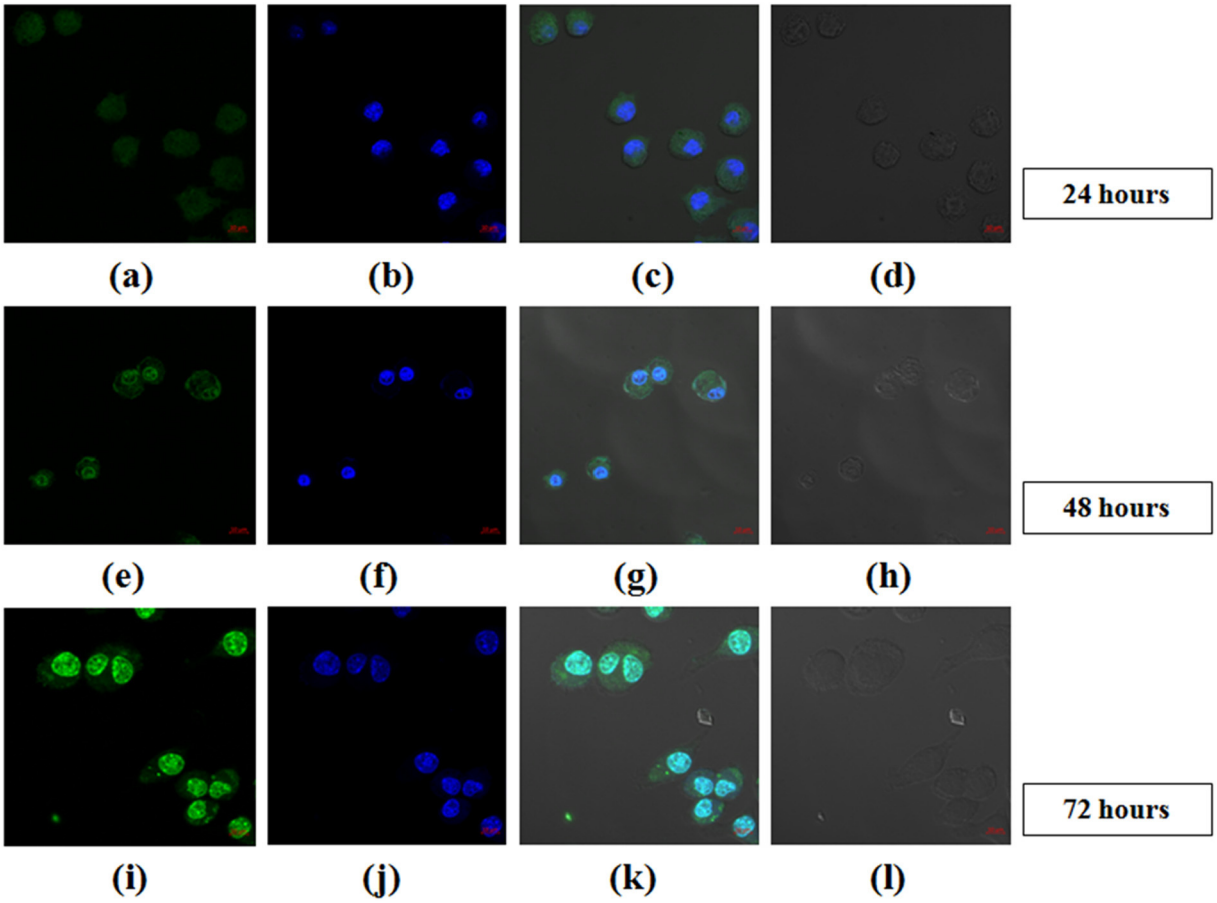

Fig. 8. Confocal microscopy images: colocalization of FITC (λ_{ex}: 488 nm) labeled VBS-AmB-SLNs after (a) 24 h, (e) 48 h, (i) 72 h of treatment; (b, f, j) DAPI (λ_{ex}: 405 nm) stained nucleus of J774A cells; (c, g, k) merged images; (d, h, l) bright field images.

release for up to 6 h shows a cumulative % release of approximately 35% was due to rapid desorption and diffusion of AmB molecules located at or close to the surface of SLNs followed by a sustained release for up to 48 h as the dominant release mechanism changed to drug diffusion [39]. The sustained release afterwards could be explained by mechanism as observed by surface renewal theory of drug dissolution which further suggests that AmB is homogenously distributed through the lipid matrix [40]. The presence of high melting point lipids along with emulsifiers in the carrier system provides an enhanced stability and allows SLNs to survive lipolysis permitting only small amount of drug to be released at regular intervals [41]. Stearic acid coated SLNs encapsulated candesartan showed sustained release pattern for extended time period to attain oral bioavailability [16]. As *Leishmania* parasite is an intra-macrophage protozoan parasite, hence to minimize toxicity to the host cell AmB is expected to release in a sustained manner.

3.7. Mucoadhesive study

Mucoadhesive study was performed for VBS-AmB-SLNs (Fig. 5) in order to get insights into the novel drug delivery platform. Oral administration is the most convenient method of drug delivery. However, mucus becomes a major barrier for achieving optimal oral mucoadhesive delivery system. SLNs should be able to interact and hence cross the mucus barrier to be able to be delivered into systemic circulation and hence achieve higher bioavailability. The SLNs should be able to adhere or bond with mucin with weak hydrogen and van der waals forces. However, because of continuous renewal of mucosal layer, mucoadhesion time is limited [42]. The turbidity of VBS-AmB-SLNs dispersion was higher when compared with that of control which could be explained by the formation of aggregates between SLNs and mucin. Due to the presence of VB_{12}, a hydrophilic molecule on the surface of SLNs, they were able to form hydrogen bonds with negatively charged mucin *i.e.* carboxyl and sulphate groups of mucin proteoglycans were able to form hydrogen bond with amide groups present in VB_{12} and hence interact with mucin. Chhonker et al. reported that due to presence of positively charged chitosan on the surface of SLNs it was able to strongly interact with negatively charged mucin [27]. Surface coating of VB_{12} and stearic acid on SLNs could be responsible for enhanced oral absorption of active drug *via* lymphatic uptake [43,44].

3.8. Stability study: in-vitro release in simulated gastro-intestinal fluid

The extreme conditions of GI tract lead to acidic and enzymatic degradation, which hampers the stability of nanoparticles. Therefore, *in vitro* release in PBS (pH 7.4) could prove to be insufficient. Simulated gastric and intestinal fluids mimics conditions present in GI tract could provide a relevant analysis of stability and release of VBS-AmB-SLNs. The % drug release of AmB was 1.57 ± 0.085% in SGF for up to 2 h and 7.6 ± 1.48% in SIF for up to 4 h as shown in Fig. 6. The orally delivered SLNs showed negligible release in SGF at low pH and small amount of drug was released in SIF at higher pH which could probably be due to the action of lipases, thereby potentially localizing their delivery to the small intestine. Presence of stearic acid in VBS-AmB-SLNs contributed to an extended stability, as pancreatic lipases do not specifically hydrolyse stearic acid. Presence of stearic acid in VBS-AmB-SLNs contributed to an extended stability, as pancreatic lipases do not specifically hydrolyse stearic acid [45]. Amekyeh et al. reported that during GI transit AmB in SLNs is absorbed slowly but significantly from the small intestines which seems to be a favourable attribute in view of

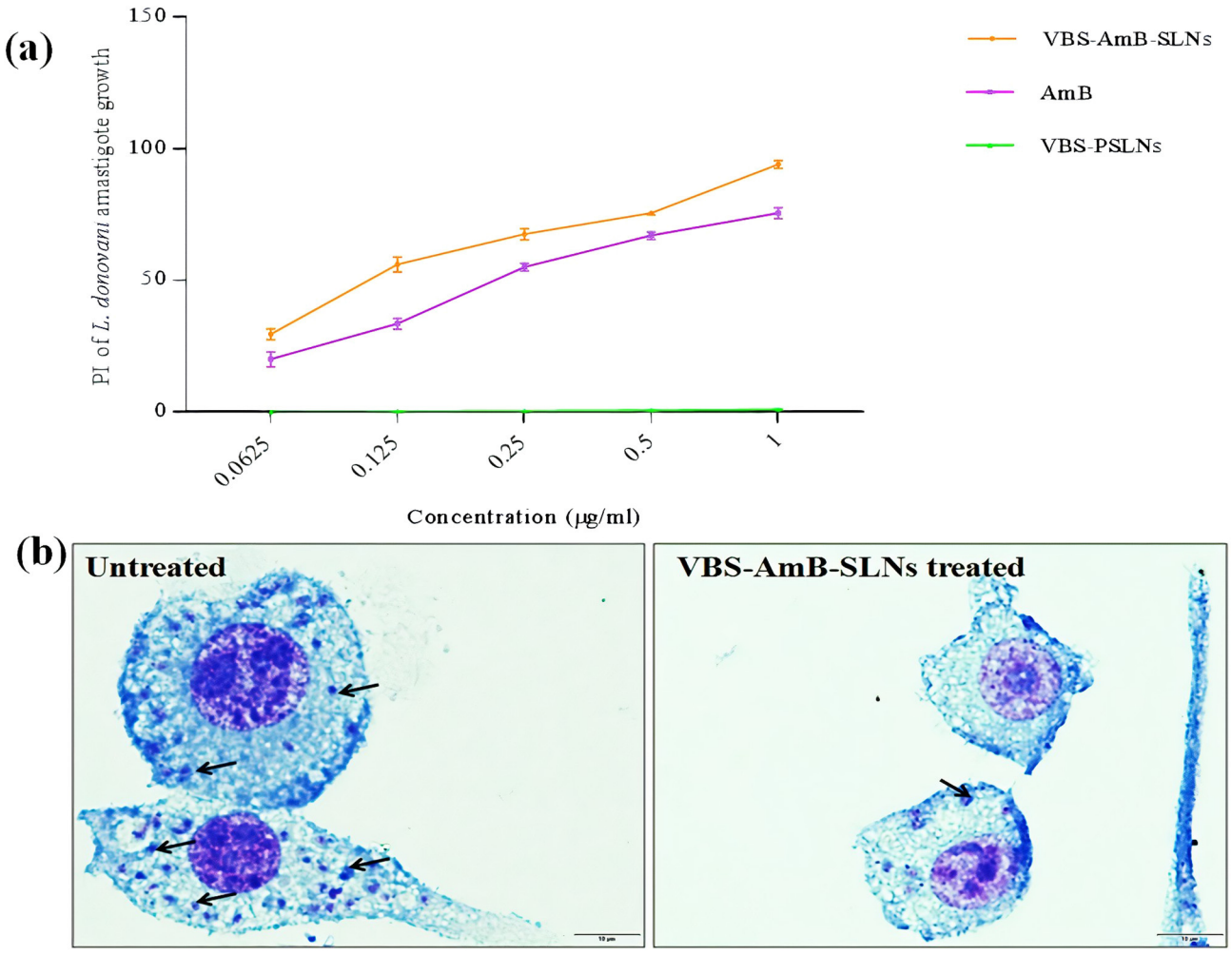

Fig. 9. (a) Percentage inhibition of VBS-AmB-SLNs, AmB and VBS-PSLNs against L. *donovani*-infected J774A.1 macrophages; (b) Microphotographs of VBS-AmB-SLNs treated and untreated L. *donovani*-infected J774A.1 macrophage. Results are presented as mean ± standard deviation.

the possible uptake of the SLNs by Peyer's patches [46].

3.9. In vitro cytotoxicity assay

To investigate the cellular viability of VBS-AmB-SLNs, MTT assay was performed on J774A.1 cells after treatment of 24 h. The results shown in Fig. 7, suggest that the percentage cell viability of VBS-AmB-SLNs were significantly higher than conventional AmB. VBS-AmB-SLNs at 5 µg/ml did not show any significant toxicity whereas the treatment with equal amount of free drug causes the cell viability to drop down to less than 80% (68%), which highlights the ability of SLNs to ameliorate the drug toxicity to the host. Even after taking VBS-AmB-SLNs with a series of increasing concentrations (0.5 µg/ml, 5 µg/ml, 50 µg/ml, 500 µg/ml) along with cell cultures, the SLNs showed significant cell viability. The CC_{50} value of VBS-AmB-SLNs was 297.34 ± 6.51 µg/ml which was fivefold higher than conventional AmB. These results demonstrate that VBS-AmB-SLNs does not impair the proliferation of J774A.1 cells, therefore elucidating their biocompatibility and non-cytotoxicity. The encapsulation of AmB in biodegradable lipid core might have resulted in lesser cytotoxicity, as the individual components of the formulation such as precirol, GMS, stearic acid and pluronic F127 have been reported to be non-cytotoxic [47–49]. It was previously reported by Muller et al. that SLNs were ten times less toxic when compared to poly-lactic acid nanoparticles in human granulocytes [50]. Also, Scholer et al. showed that SLNs neither caused cytotoxicity nor led to secretion of pro-inflammatory cytokines by murine peritoneal macrophages confirming the biocompatibility of SLNs [51].

3.10. Cellular uptake study

As *Leishmania* amastigotes reside inside host's macrophages, therefore the cellular uptake of SLNs was an important factor to evaluate its therapeutic efficiency. Hence, we investigated the cellular uptake of FITC labeled VBS-AmB-SLNs in J774A.1 cells with exposure time of 24, 48 and 72 h respectively (Fig. 8) by confocal microscopy. A major step in cellular uptake is interaction with the cell membrane and subsequent endocytosis leading to engulfment of SLNs. Depending upon the cell type *i.e.* macrophages where VB_{12} enhances the rate of phagocytosis as reported previously as well as the presence of VB_{12} on the surface of SLNs leads to enhanced uptake of VBS-AmB-SLNs due to receptor mediated endocytosis and uptake pathway present intrinsically in our body [52]. AmB has been reported to exhibit higher partition coefficients when stearic acid was selected for the preparation of SLNs [35]. Also, saturated fatty acids with high melting point showed high permeation rate across the biological membranes and VB_{12} was an effective targeting agent for nanoparticles which resulted in enhanced uptake of nanoparticles from the intestinal loops [54,55].

3.11. Anti-leishmanial activity of VBS-AmB-SLNs against L. donovani-infected J774A.1 macrophages, in vitro

Inhibition of amastigote growth in intracellular macrophages by

VBS-AmB-SLNs, VBS-PSLNs and AmB was evaluated. All samples were stained and the intra-cellular amastigote growth was determined. VBS-AmB-SLNs (1 μg/ml) significantly ($P < 0.01$) reduced intra-cellular amastigotes compared to free AmB (Fig. 9(a) & (b)). The IC_{50} value of VBS-AmB-SLNs (0.127809 ± 0.012227 μg/ml) was higher than the IC_{50} values of free AmB (0.38365 ± 0.037201 μg/ml). VBS-AmB-SLNs (1 μg/ml) showed maximum percentage of inhibition (94%) on intra-cellular amastigote growth of L. *donovani* as compared to conventional AmB (75.5%). The enhanced activity against *Leishmania* parasite is ascribed to VB_{12}-stearic acid conjugate which aids in increased internalization by receptor mediated endocytosis in the infected macrophages, leading to augmented parasite killing [19,55–57].

4. Conclusions

In the current study, a novel nanoparticulate drug delivery system was developed by a combination of double emulsion solvent evaporation and thermal sensitive hydrogel techniques, VBS-AmB-SLNs for the increased oral delivery of AmB. The particle size distribution indicated homogeneity of synthesized SLNs with a net neutral charge on SLNs favouring higher mucus permeating ability, and hence can enhance the oral bioavailability of AmB. Indeed, VBS-AmB-SLNs conferred complete internalization within the macrophage cells. *In vitro* studies showed lower cytotoxicity against J774A.1 cells and higher chemical stability against digestive enzymes. Further, mucoadhesive study confirmed the interaction of VBS-AmB-SLNs with mucin. Finally, anti-leishmanial evaluation against intramacrophage amastigotes showed an enhanced efficacy (94%) over conventional AmB (75.5%). In order to endorse these results and to corroborate and evaluate if such delivery systems increase AmB oral bioavailability, preclinical *in vivo* studies are envisaged.

Supplementary data to this article can be found online at https://doi.org/10.1016/j.msec.2020.111279.

Funding

Aakriti Singh and Shabi Parvez thank Institute of Nano Science and Technology for the Doctoral Fellowship. Ganesh Yadagiri is thankful to Department of Science & Technology (DST) for providing financial support. This work is supported by Government of India for funding under DST-SERB Early Career Research Award (ECR/2016/000977) and in part by DST-Nano Mission (SR/NM/NS-57/2016).

CRediT authorship contribution statement

Aakriti Singh:Methodology, Software, Data curation, Writing - original draft, Visualization, Investigation, Writing - review & editing.**Ganesh Yadagiri**:Methodology, Software, Data curation, Writing - original draft, Visualization, Investigation, Writing - review & editing.**Shabi Parvez**:Methodology, Software, Data curation, Writing - original draft, Visualization, Investigation, Writing - review & editing.**Om Prakash Singh**:Methodology, Software, Data curation, Writing - original draft, Visualization, Investigation, Writing - review & editing.**Anurag Verma**:Methodology, Software, Data curation, Writing - original draft, Visualization, Investigation, Writing - review & editing.**Shyam Sundar**:Methodology, Software, Data curation, Writing - original draft, Visualization, Investigation, Writing - review & editing.**Shyam Lal Mudavath**:Methodology, Software, Data curation, Writing - original draft, Visualization, Investigation, Writing - review & editing, Conceptualization, Funding acquisition, Supervision.

Declaration of competing interest

The authors declare that they have no known competing financial interests or personal relationships that could have appeared to influence the work reported in this paper.

References

[1] G. Yadagiri, P.P. Singh, Chemotherapy and experimental models of visceral leishmaniasis, Infect. Dis. Your Heal, Springer Singapore, 2018, pp. 63–97, , https://doi.org/10.1007/978-981-13-1577-0_5.
[2] Leishmaniasis, (n.d.). https://www.who.int/news-room/fact-sheets/detail/leishmaniasis (accessed June 5, 2020).
[3] L. Monzote, Current Treatment of Leishmaniasis: A Review, (2009).
[4] N. Tiwari, M.R. Gedda, V.K. Tiwari, S.P. Singh, R.K. Singh, Limitations of current therapeutic options, possible drug targets and scope of natural products in control of leishmaniasis, Mini-Rev. Med. Chem. 18 (2017), https://doi.org/10.2174/1389557517666170425105129.
[5] S. Mohapatra, Drug resistance in leishmaniasis: newer developments, Trop. Parasitol. 4 (2014) 4, https://doi.org/10.4103/2229-5070.129142.
[6] A. Chattopadhyay, M. Jafurulla, A novel mechanism for an old drug: amphotericin B in the treatment of visceral leishmaniasis, Biochem. Biophys. Res. Commun. 416 (2011) 7–12, https://doi.org/10.1016/j.bbrc.2011.11.023.
[7] S. Sundar, J. Jaya, Liposomal amphotericin B and leishmaniasis: dose and response, J. Global Infect. Dis. 2 (2010) 159, https://doi.org/10.4103/0974-777x.62886.
[8] R.J. Hamill, Amphotericin B formulations: a comparative review of efficacy and toxicity, Drugs 73 (2013) 919–934, https://doi.org/10.1007/s40265-013-0069-4.
[9] J.J. Torrado, D.R. Serrano, I.F. Uchegbu, The oral delivery of amphotericin B, Ther. Deliv. 4 (2013) 9–12, https://doi.org/10.4155/tde.12.134.
[10] J.J. Torrado, R. Espada, M.P. Ballesteros, S. Torrado-Santiago, Amphotericin B formulations and drug targeting, J. Pharm. Sci. 97 (2008) 2405–2425, https://doi.org/10.1002/jps.21179.
[11] M. Ching, K. Raymond, R. Bury, M. Mashford, D. Morgan, Absorption of orally administered amphotericin B lozenges, Br. J. Clin. Pharmacol. 16 (1983) 106–108, https://doi.org/10.1111/j.1365-2125.1983.tb02152.x.
[12] S.L. Mudavath, M. Talat, M. Rai, O.N. Srivastava, S. Sundar, Characterization and evaluation of amine-modified graphene amphotericin B for the treatment of visceral leishmaniasis: in vivo and in vitro studies, Drug Des. Devel. Ther. 8 (2014) 1235–1247, https://doi.org/10.2147/DDDT.S63994.
[13] O.P. Singh, M.R. Gedda, S.L. Mudavath, O.N. Srivastava, S. Sundar, Envisioning the innovations in nanomedicine to combat visceral leishmaniasis: for future theranostic application, Nanomedicine 14 (2019) 1911–1927, https://doi.org/10.2217/nnm-2018-0448.
[14] P. Chaubey, B. Mishra, S.L. Mudavath, R.R. Patel, S. Chaurasia, S. Sundar, V. Suvarna, M. Monteiro, Mannose-conjugated curcumin-chitosan nanoparticles: efficacy and toxicity assessments against Leishmania donovani, Int. J. Biol. Macromol. 111 (2018) 109–120, https://doi.org/10.1016/j.ijbiomac.2017.12.143.
[15] H. Ali, S.K. Singh, Biological voyage of solid lipid nanoparticles: a proficient carrier in nanomedicine, Ther. Deliv. 7 (2016) 691–709, https://doi.org/10.4155/tde-2016-0038.
[16] A. Mahajan, S. Kaur, Design, formulation, and characterization of stearic acid-based solid lipid nanoparticles of candesartan cilexetil to augment its oral bioavailability, Asian J. Pharm. Clin. Res. 11 (2018) 344–350, https://doi.org/10.22159/ajpcr.2018.v11i4.23849.
[17] Z.H. Zhang, Y.L. Zhang, J.P. Zhou, H.X. Lv, Solid lipid nanoparticles modified with stearic acid-octaarginine for oral administration of insulin, Int. J. Nanomedicine 7 (2012) 3333–3339, https://doi.org/10.2147/IJN.S31711.
[18] S. Kumar, J.K. Randhawa, Solid lipid nanoparticles of stearic acid for the drug delivery of paliperidone, RSC Adv. 5 (2015) 68743–68750, https://doi.org/10.1039/c5ra10642g.
[19] A. Verma, S. Sharma, P.K. Gupta, A. Singh, B.V. Teja, P. Dwivedi, G.K. Gupta, R. Trivedi, P.R. Mishra, Vitamin B12 functionalized layer by layer calcium phosphate nanoparticles: a mucoadhesive and pH responsive carrier for improved oral delivery of insulin, Acta Biomater. 31 (2016) 288–300, https://doi.org/10.1016/j.actbio.2015.12.017.
[20] G.J. Russell-Jones, S.W. Westwood, A.D. Habberfield, Vitamin B12 mediated oral delivery systems for granulocyte-colony stimulating factor and erythropoietin, Bioconjug. Chem. 6 (1995) 459–465, https://doi.org/10.1021/bc00034a016.
[21] G.J. Russell-Jones, S.W. Westwood, P.G. Farnworth, J.K. Findlay, H.G. Burger, Synthesis of LHRH antagonists suitable for oral administration via the vitamin B12 uptake system, Bioconjug. Chem. 6 (1995) 34–42, https://doi.org/10.1021/bc00031a600.
[22] G.J. Russell-Jones, The potential use of receptor-mediated endocytosis for oral drug delivery, Adv. Drug Deliv. Rev. 20 (1996) 83–97, https://doi.org/10.1016/0169-409X(95)00131-P.
[23] A.K. Petrus, T.J. Fairchild, R.P. Doyle, Traveling the vitamin B12 pathway: oral delivery of protein and peptide drugs, Angew. Chem. Int. Ed. Eng. 48 (2009) 1022–1028, https://doi.org/10.1002/anie.200800865.
[24] R. Fowler, D. Vllasaliu, F.H. Falcone, M. Garnett, B. Smith, H. Horsley, C. Alexander, S. Stolnik, Uptake and transport of B12-conjugated nanoparticles in airway epithelium, J. Control. Release 172 (2013) 374–381, https://doi.org/10.1016/j.jconrel.2013.08.028.
[25] Y. Wang, B.A. Aleiwi, Q. Wang, M. Kurosu, Selective esterifications of primary alcohols in a water-containing solvent, Org. Lett. 14 (2012) 4910–4913, https://doi.org/10.1021/ol3022337.
[26] R. Yang, R.C. Gao, C.F. Cai, H. Xu, F. Li, H.B. He, X. Tang, Preparation of gel-core-solid lipid nanoparticle: a novel way to improve the encapsulation of protein and

peptide, Chem. Pharm. Bull. 58 (2010) 1195–1202, https://doi.org/10.1248/cpb.58.1195.
[27] Y.S. Chhonker, Y.D. Prasad, H. Chandasana, A. Vishvkarma, K. Mitra, P.K. Shukla, R.S. Bhatta, Amphotericin-B entrapped lecithin/chitosan nanoparticles for prolonged ocular application, Int. J. Biol. Macromol. 72 (2015) 1451–1458, https://doi.org/10.1016/j.ijbiomac.2014.10.014.
[28] S. Klein, The use of biorelevant dissolution media to forecast the in vivo performance of a drug, AAPS J. 12 (2010) 397–406, https://doi.org/10.1208/s12248-010-9203-3.
[29] H. Yuan, J. Chen, Y.Z. Du, F.Q. Hu, S. Zeng, H.L. Zhao, Studies on oral absorption of stearic acid SLN by a novel fluorometric method, Colloids Surf. B: Biointerfaces 58 (2007) 157–164, https://doi.org/10.1016/j.colsurfb.2007.03.002.
[30] D.C. de O. Nunes, L.B. Bispo-da-Silva, D.R. Napolitano, M.S. Costa, M.M.N.R. Figueira, R.S. Rodrigues, V. de M. Rodrigues, K.A.G. Yoneyama, In vitro additive interaction between ketoconazole and antimony against intramacrophage Leishmania (Leishmania) amazonensis amastigotes, PLoS One 12 (2017) e0180530, https://doi.org/10.1371/journal.pone.0180530.
[31] H. He, P. Wang, C. Cai, R. Yang, X. Tang, VB12-coated gel-core-SLN containing insulin: another way to improve oral absorption, Int. J. Pharm. 493 (2015) 451–459, https://doi.org/10.1016/j.ijpharm.2015.08.004.
[32] Z. Yu, W. Fan, L. Wang, J. Qi, Y. Lu, W. Wu, Effect of surface charges on oral absorption of intact solid lipid nanoparticles, Mol. Pharm. (2019), https://doi.org/10.1021/acs.molpharmaceut.9b00861.
[33] G. Rizzo, A.S. Laganà, A.M. Chiara Rapisarda, G.M. Grazia, L. Ferrera, M. Buscema, P. Rossetti, A. Nigro, V. Muscia, G. Valenti, F. Sapia, G. Sarpietro, M. Zigarelli, S.G. Vitale, Vitamin B12 Among Vegetarians: Status, Assessment and Supplementation, (2016), https://doi.org/10.3390/nu8120767.
[34] G. Schwartzman, I. Asher, V. Folen, W. Brannon, J. Taylor, Ambiguities in IR and X-ray characterization of amphotericin B, J. Pharm. Sci. 67 (1978) 398–400, https://doi.org/10.1002/jps.2600670334.
[35] F. Kesisoglou, M. Wang, K. Galipeau, P. Harmon, G. Okoh, W. Xu, Effect of amorphous nanoparticle size on bioavailability of anacetrapib in dogs, J. Pharm. Sci. 108 (2019) 2917–2925, https://doi.org/10.1016/j.xphs.2019.04.006.
[36] D.T. Friesen, R. Shanker, M. Crew, D.T. Smithey, W.J. Curatolo, J.A.S. Nightingale, Hydroxypropyl methylcellulose acetate succinate-based spray-dried dispersions: an overview, Mol. Pharm. 5 (2008) 1003–1019, https://doi.org/10.1021/mp8000793.
[37] D. Lombardo, P. Calandra, D. Barreca, S. Magazù, M.A. Kiselev, Soft interaction in liposome nanocarriers for therapeutic drug delivery, Nanomaterials 6 (2016), https://doi.org/10.3390/nano6070125.
[38] R. Cavalli, O. Caputo, M.R. Gasco, Solid lipospheres of doxorubicin and idarubicin, Int. J. Pharm. 89 (1993) R9–R12, https://doi.org/10.1016/0378-5173(93)90313-5.
[39] E. Palma, A. Pasqua, A. Gagliardi, D. Britti, M. Fresta, D. Cosco, Antileishmanial activity of amphotericin B-loaded-PLGA nanoparticles: an overview, Materials (Basel) 11 (2018), https://doi.org/10.3390/ma11071167.
[40] H. Baishya, Application of mathematical models in drug release kinetics of carbidopa and levodopa ER tablets, J. Dev. Drugs 06 (2017) 1–8, https://doi.org/10.4172/2329-6631.1000171.
[41] Z. Yu, W. Fan, L. Wang, H. He, Y. Lv, J. Qi, Y. Lu, W. Wu, Slowing down lipolysis significantly enhances the oral absorption of intact solid lipid nanoparticles, Biomater. Sci. 7 (2019) 4273–4282, https://doi.org/10.1039/c9bm00873j.
[42] S.K. Lai, Y.Y. Wang, J. Hanes, Mucus-penetrating nanoparticles for drug and gene delivery to mucosal tissues, Adv. Drug Deliv. Rev. 61 (2009) 158–171, https://doi.org/10.1016/j.addr.2008.11.002.
[43] S. Banerjee, A. Kundu, Lipid-drug conjugates: a potential nanocarrier system for oral drug delivery applications, Daru 26 (2018) 65–75, https://doi.org/10.1007/s40199-018-0209-1.
[44] K.B. Taylor, J.E. French, The role of the lymphatics in the intestinal absorption of vitamin B12 in the rat, Q. J. Exp. Physiol. Cogn. Med. Sci. 45 (1960) 72–76, https://doi.org/10.1113/expphysiol.1960.sp001445.
[45] M. Sugano, Y. Imasato, M. Nakayama, K. Imaizumi, Lymphatic transport of stearic acid and its effect on cholesterol transport in rats, J. Nutr. Sci. Vitaminol. (Tokyo) 40 (1994) 275–282, https://doi.org/10.3177/jnsv.40.275.
[46] H. Amekyeh, N. Billa, K.H. Yuen, S.L.S. Chin, A gastrointestinal transit study on amphotericin B-loaded solid lipid nanoparticles in rats, AAPS PharmSciTech 16 (2015) 871–877, https://doi.org/10.1208/s12249-014-0279-4.
[47] R.M.P. Gutierrez, J.V.M. Mendez, I.A. Vazquez, A novel approach to the oral delivery of bionanostructures for systemic disease, Nanostructures Oral Med, Elsevier Inc., 2017, pp. 27–59, , https://doi.org/10.1016/B978-0-323-47720-8.00002-X.
[48] E. Ruel-Gariépy, J.-C. Leroux, In situ-forming hydrogels—review of temperature-sensitive systems, Eur. J. Pharm. Biopharm. 58 (2004) 409–426, https://doi.org/10.1016/j.ejpb.2004.03.019.
[49] D. Sutaria, B.K. Grandhi, A. Thakkar, J. Wang, S. Prabhu, Chemoprevention of pancreatic cancer using solid-lipid nanoparticulate delivery of a novel aspirin, curcumin and sulforaphane drug combination regimen, Int. J. Oncol. 41 (2012) 2260–2268, https://doi.org/10.3892/ijo.2012.1636.
[50] R.H. Müller, S. Maaßen, H. Weyhers, W. Mehnert, Phagocytic uptake and cytotoxicity of solid lipid nanoparticles (SLN) sterically stabilized with poloxamine 908 and poloxamer 407, J. Drug Target. 4 (1996) 161–170, https://doi.org/10.3109/10611869609015973.
[51] N. Schöler, E. Zimmermann, U. Katzfey, H. Hahn, R.H. Müller, O. Liesenfeld, Preserved solid lipid nanoparticles (SLN) at low concentrations do cause neither direct nor indirect cytotoxic effects in peritoneal macrophages, Int. J. Pharm. 196 (2000) 235–239, https://doi.org/10.1016/S0378-5173(99)00430-5.
[52] K.G. Thomaskutty, C.M. Lee, Interaction of nutrition and infection: macrophage activity in vitamin B12-deficient rats infected with Trypanosoma lewisi, J. Natl. Med. Assoc. 79 (1987) 441–446 http://www.ncbi.nlm.nih.gov/pubmed/3295263 , Accessed date: 6 June 2020.
[54] G. Russell-Jones, Intestinal receptor targeting for peptide delivery: an expert's personal perspective on reasons for failure and new opportunities, Ther. Deliv. 2 (2011) 1575–1593, https://doi.org/10.4155/tde.11.129.
[55] M.J. Kim, H.J. Doh, M.K. Choi, S.J. Chung, C.K. Shim, D.D. Kim, J.S. Kim, C.S. Yong, H.G. Choi, Skin permeation enhancement of diclofenac by fatty acids, Drug Deliv. 15 (2008) 373–379, https://doi.org/10.1080/10717540802006898.
[56] B. Seetharam, Recptor-mediated endocytosis of cobalamine (vitamin B_{12}), Annu. Rev. Nutr. 19 (1999) 173–195, https://doi.org/10.1146/annurev.nutr.19.1.173.
[57] Y.Z. Du, L.L. Cai, J. Li, M.D. Zhao, F.Y. Chen, H. Yuan, F.Q. Hu, Receptor-mediated gene delivery by folic acid-modified stearic acid-grafted chitosan micelles, Int. J. Nanomedicine 6 (2011) 1559–1568, https://doi.org/10.2147/ijn.s23828.
[58] M. Gharagozlou, R. Bayati, Photocatalytic characteristics of single phase Fe-doped anatase TiO2 nanoparticles sensitized with vitamin B12, Mater. Res. Bull. 61 (2015) 340–347, https://doi.org/10.1016/j.materresbull.2014.10.043.
[59] S.M. Sadeghzadeh, R. Zhiani, S. Emrani, KCC-1/GMSI/VB12 as a new nano catalyst for the carbonylative Suzuki-Miyaura crosscoupling reaction, RSC Adv. 7 (2017) 32139–32145, https://doi.org/10.1039/c7ra06021a.
[60] K.S. Taraszka, E. Chen, T. Metzger, M.R. Chance, Identification of Structural Markers for Vitamin b12 and Other Corrinoid Derivatives in Solution Using Ftir Spectroscopy, Biochemistry. 30 (1991) 1222–1227, https://doi.org/10.1021/bi00219a009.
[61] V. Jain, A. Gupta, V.K. Pawar, S. Asthana, A.K. Jaiswal, A. Dube, M.K. Chourasia, Chitosan-Assisted Immunotherapy for Intervention of Experimental Leishmaniasis via Amphotericin B-Loaded Solid Lipid Nanoparticles, Appl. Biochem. Biotechnol. 174 (2014) 1309–1330, https://doi.org/10.1007/s12010-014-1084-y.